ELSEVIER

Surface Science 410 (1998) 214–227

surface science

TPD, HREELS and UPS study of the adsorption and reaction of methyl nitrite (CH_3ONO) on Pt(111)

John W. Peck, Daniel I. Mahon, David E. Beck, Barbara Bansenaur 1, Bruce E. Koel *

Department of Chemistry, University of Southern California, Los Angeles, CA 90089-0482, USA

Received 17 July 1997; accepted for publication 16 March 1998

Abstract

The adsorption and reaction of methyl nitrite (CH_3ONO, CD_3ONO) on Pt(111) was studied using HREELS, UPS, TPD, AES, and LEED. Adsorption of methyl nitrite on Pt(111) at 105 K forms a chemisorbed monolayer with a coverage of 0.25 ML, a physisorbed second layer with the same coverage that desorbs at 134 K, and a condensed multilayer that desorbs at 117 K. The Pt(111) surface is very reactive towards chemisorbed methyl nitrite; adsorption in the monolayer is completely irreversible. CH_3ONO dissociates to form NO and an intermediate which subsequently decomposes to yield CO and H_2 at low coverages and methanol for CH_3ONO coverages above one-half monolayer. We propose that a methoxy intermediate is formed. At least some C–O bond breaking occurs during decomposition to leave carbon on the surface after TPD. UPS and HREELS show that some methyl nitrite decomposition occurs below 110 K and all of the methyl nitrite in the monolayer is decomposed by 165 K. Intermediates from methyl nitrite decomposition are also relatively unstable on the Pt(111) surface since coadsorbed NO, CO and H are formed below 225 K.

Keywords: Auger electron spectroscopy (AES); Chemisorption; Low energy electron diffraction (LEED); Low index single crystal surfaces; Methylnitrite; Platinum; Thermal desorption spectroscopy; Visible and ultraviolet photoelectron spectroscopy

1. Introduction

Methyl nitrite (CH_3ONO) is a very reactive molecule in the gas phase because of the weak O–NO bond (O–NO = 42 kcal/mol [1]). Our interest in exploring the reactions of this molecule on surfaces too comes from its potential importance as an intermediate in the dissociation of adsorbed CH_3NO_2 [1–7] and the possibility that methyl nitrite can be used as an adsorbed precursor for preparing surface methoxy species.

Only two previous studies have been made of the chemistry of methyl nitrite on transition metal surfaces, i.e. on Au(111) [8] and Ag(111) [9]. Both surfaces are too inert to activate bond dissociation in UHV and no thermal reaction was observed in TPD. Pressley et al. [9] also investigated the electron induced dissociation (EID) of methyl nitrite adsorbed on Ag(111) and found that reaction proceeds preferentially through cleavage of the O–N bond to yield formaldehyde, water and methane. Recently, we also used TPD to investigate the adsorption and reaction of methyl nitrite on two Sn/Pt(111) surface alloys [10,11]. Adsorption was 30–40% reversible, and reaction proceeded via dissociation of the O–NO bond to

* Corresponding author. Fax: +1 213 7403972; e-mail: koel@chem1.usc.edu

1 Present address: Department of Chemistry, University of Wisconsin, Eau Claire, WI 54702-4004, USA.

0039-6028/98/$19.00
PII: S0039-6028(98)00284-2

form NO and a large concentration of adsorbed methoxy species which were stable up to ~300 K on the Pt–Sn alloy surfaces.

In this paper, we report on studies of the adsorption and reaction of methyl nitrite on Pt(111). We find that methyl nitrite is much more reactive on Pt(111) than nitromethane [12], and Pt(111) completely irreversibly chemisorbs methyl nitrite. CH_3ONO decomposes during TPD to form NO, CO, H_2 and CH_3OH. HREELS and UPS indicate that some O–NO bond cleavage occurs at 110 K, and subsequent intermediates are completely decomposed below 225 K.

2. Experimental methods

The experiments were performed in two separate stainless steel UHV chambers. Both were equipped with instrumentation for Auger electron spectroscopy (AES), low energy electron diffraction (LEED), Ar^+ ion sputtering, and a shielded UTI 100C quadrupole mass spectrometer (QMS) for temperature programmed desorption (TPD). The system base pressure for the TPD studies was 5×10^{-11} Torr. Additionally, the second chamber had instrumentation for high resolution electron energy loss spectroscopy (HREELS) and ultraviolet photoelectron spectroscopy (UPS).

AES spectra were recorded using a Perkin-Elmer (15-255G) double-pass cylindrical mirror analyzer (CMA). UPS spectra using He(II) (40.84 eV) photon energies were taken using the CMA in a retarding mode at 25 eV pass energy (0.40 eV resolution). LEED was carried out using Perkin-Elmer (15-180) LEED optics. The McAllister HREELS spectrometer was constructed of single 127° cylindrical sectors for both the monochromator and analyzer, and the control electronics utilized a stable, low noise design [13]. Spectra were taken with the sample at 110–115 K, with a typical resolution of ~75 cm^{-1}, a count rate of 5–35 kcps, and an incident beam energy of 3 eV. All TPD measurements are made using the QMS ionizer in line-of-sight to the sample surface with a linear heating rate of ~4 K/s. The crystal was positioned ~1 mm from the entrance aperture of the QMS shield to reduce contributions to the spectra from the crystal back and edges [14]. A highly transparent, fine Ni screen was placed over the end of the ionizer grid (biased at −55 V) on the QMS and over the shield entrance (grounded) to eliminate possible damage to the adsorbed layer from low energy electrons coming from the QMS ionizer region [15].

The Pt(111) crystal was cooled to 95 K using liquid nitrogen or resistively heated to 1200 K. The temperature was recorded by a chromel–alumel thermocouple spot welded to the side of the crystal. The Pt(111) surface was cleaned by a combination of Ar^+ ion sputtering, annealing in vacuum, and oxygen treatments. Ion bombardment of the crystal was carried out using 1 kV Ar^+ (3×10^{-5} Torr Ar) for 5–10 min with the sample at 800 K, and then the crystal was annealed to 1000 K in UHV to reorder the surface. Oxygen treatments at 2×10^{-8} Torr O_2 for 5–10 min with the crystal at 800–1000 K, followed by flashing in vacuum to 1000 K, were used to remove submonolayer coverages of surface carbon.

Methyl nitrite was prepared from methanol-d_4, D_2O, D_2SO_4, and HSO_3ONO according to an accepted procedure [16] and purified by three successive distillations at −25°C under a nitrogen flow through a standard glass distillation column. The sample was further purified to remove gaseous impurities using freeze–pump–thaw cycles. The purity was checked using both IR [17] and in situ mass spectrometry.

Gas exposures for the TPD studies were given with the sample below 100 K, and for the HREELS and UPS studies below 110 K. Exposures given in this paper are in units of Langmuirs (10^{-6} Torr s) after the measured values were multiplied by a factor to account for the multicapillary array doser enhancement. The doser correction factor was obtained by comparing uptake curves from exposures produced by the directed beam doser with those from background exposures.

3. Results

3.1. Adsorption and reaction of methyl nitrite

Methyl nitrite TPD spectra following CH_3ONO adsorption on the Pt(111) surface are shown in

Fig. 1. Up to an exposure of 0.18 L, no methyl nitrite desorption was observed. As the exposure was increased a peak appeared at 134 K. This peak saturated and a new peak grew in at 117 K as the exposure was increased further. This lower temperature peak did not saturate with increased exposures and thus it is associated with desorption of multilayers of physisorbed methyl nitrite. This multilayer desorption temperature is identical to that on the Ag(111) surface [9].

Signals at 58, 56, 54, 46, 44, 43, 32–27, 18, 17, 16, 12 and 2 AMU were monitored during TPD to watch for gas phase products from methyl nitrite decomposition. Signals at 32, 30 and 29 AMU were used to assess desorption of methanol (CH_3OH), NO, and formaldehyde (CH_2O). Mass 46 was used to detect a possible NO_2 product. Fig. 2 shows TPD data for the reaction products of CH_3ONO on Pt(111). The two low temperature desorption states of CH_3ONO at 134 and 117 K are seen in the 61, 30, 29, 28 and 2 AMU channels. A peak at 190 K was seen for mass 32 (and 31, not shown) that we assign to methanol. TPD at 30 AMU shows that NO desorbs in peaks at 320 and 355 K. A small peak was observed at ~240 K in the 30, 29 and 28 AMU channels that we assign to formaldehyde. Finally, CO desorbs in a sharp peak at 450 K and a broad feature at 575 K, and H_2 desorbs at 260 K. Later in this section we discuss our rationale for these assignments.

Adsorption kinetics (uptake) plots of methyl nitrite and the major decomposition products were constructed from TPD peak areas. Fig. 3 shows

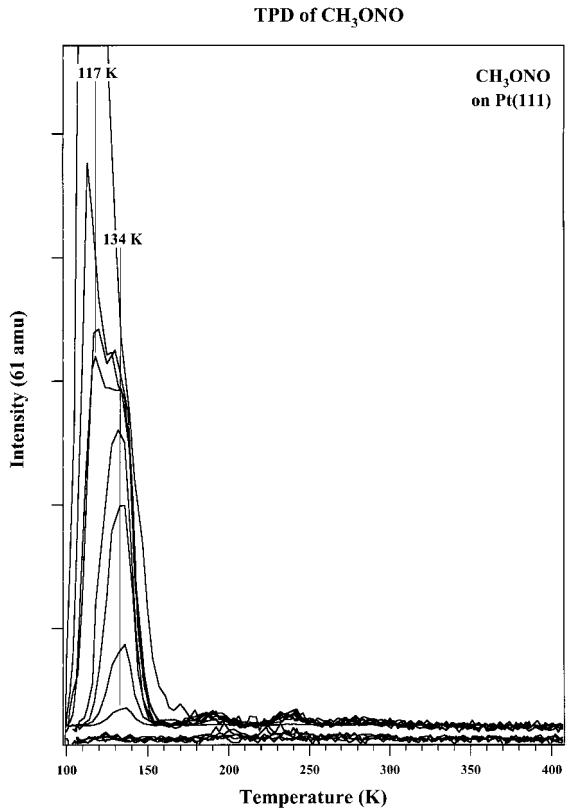

Fig. 1. CH_3ONO TPD spectra after CH_3ONO exposures on the Pt(111) surface at 95 K. Exposures used were: 0.005, 0.010, 0.050, 0.10, 0.15, 0.20, 0.24, 0.30, 0.40, 0.50, 0.60, 0.80, and 1.0 L.

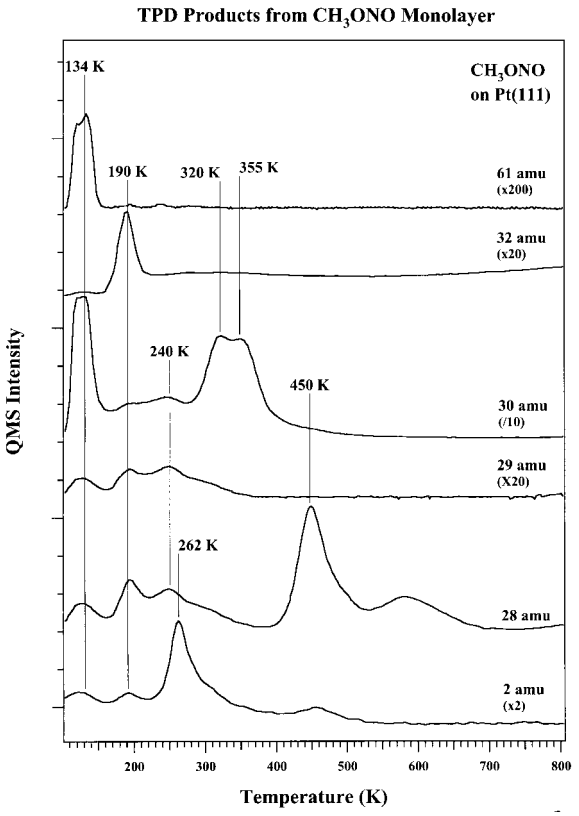

Fig. 2. TPD spectra of products from the reaction of CH_3ONO on Pt(111). CH_3ONO was dosed on the Pt(111) surface to a coverage exceeding one monolayer.

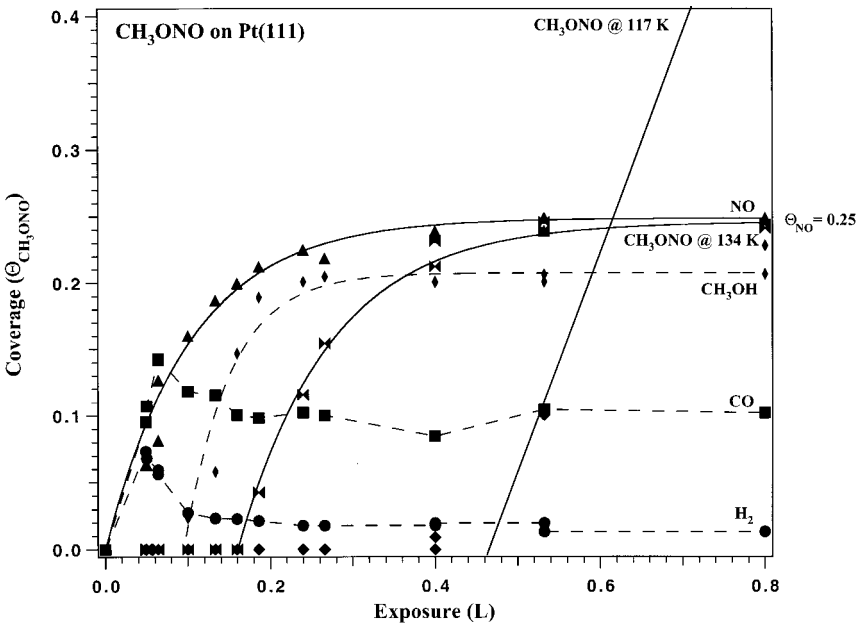

Fig. 3. Uptake curve for CH_3ONO adsorption kinetics constructed from TPD results after adsorption of CH_3ONO on the Pt(111) surface at 95 K. The amount of NO desorbed from the reaction of CH_3ONO is 0.25 ML, which represents 100% of the total monolayer coverage of CH_3ONO.

that at low exposures, only H_2, CO, and NO products desorb. Methanol desorption begins at ~0.1 L after the monolayer is about one-half filled. All of these peaks saturate at ~0.2 L, and CH_3ONO desorption is seen for the first time at 134 K. Increasing exposures saturate this peak at ~0.4 L and increase the size of the low temperature (multilayer) CH_3ONO peak at 117 K.

The coverages of NO and CH_3ONO corresponding to the desorption peak areas are calibrated in absolute units of CH_3ONO coverage. This was done by first calibrating the NO desorption area to the known coverage $H_{NO} = 0.50$ ML from NO exposure on Pt(111) [18], and then using a one-to-one correspondence for the amount of CH_3ONO decomposition to NO yield. The CH_3ONO area was calibrated to CH_3ONO coverage by forcing the uptake curve to have a constant slope, i.e. constant sticking coefficient, for the region at low coverage where the NO yield reflects the CH_3ONO coverage since there is no CH_3ONO desorption, and the region at high coverage where CH_3ONO is the only desorbed species. The CH_3OH, CO, and H_2 yields in Fig. 3 are not calibrated to CH_3ONO coverage, but do correlate with the NO yield from CH_3ONO decomposition.

No CH_3ONO desorbs until the evolution of all of the decomposition products has stopped. The coverage of CH_3ONO that undergoes decomposition is 0.25 ML. This is the coverage of CH_3ONO in the chemisorbed monolayer based on several other observations. The reported monolayer coverage of methyl nitrite on Ag(111) is 0.3 ML [9] and the monolayer coverage on two Pt–Sn surface alloys that show partially reversible chemisorption is 0.26 ML [11].

The methyl nitrite peak at 134 K was observed in previous experiments for methyl nitrite adsorption on Ag(111) [9] and was associated with a weakly chemisorbed state of methyl nitrite adsorbed in the monolayer. The uptake curves produced in this experiment, and on the Pt–Sn surface alloys [11], show that this state of methyl nitrite desorbing at 134 K has a coverage of ~0.25 ML, equal in coverage to the chemisorbed monolayer, and so this state should be associated with a second, physisorbed layer on top of the monolayer on Pt(111).

TPD spectra showing NO evolution from the dissociation of methyl nitrite on Pt(111) for a series of initial CH_3ONO coverages are shown in Fig. 4. At low coverages, only the highest temperature NO state was present, however, near monolayer coverage the peak at 320 K appeared.

The NO desorption above 300 K in Fig. 4 agrees well with the NO TPD spectra after NO exposures from the work of Xu and Koel [18], indicating NO desorption from the dissociation of methyl nitrite is desorption rate-limited. NO peaks at 320 and 360 K can be assigned to desorption from bridging and atop sites, respectively [18].

Fig. 5 provides coverage-dependent TPD spectra for H_2, CO and CH_3OH desorption from CH_3ONO decomposition on Pt(111). TPD spectra, obtained at 2 AMU to monitor H_2 for a series of increasing CH_3ONO exposures, are shown

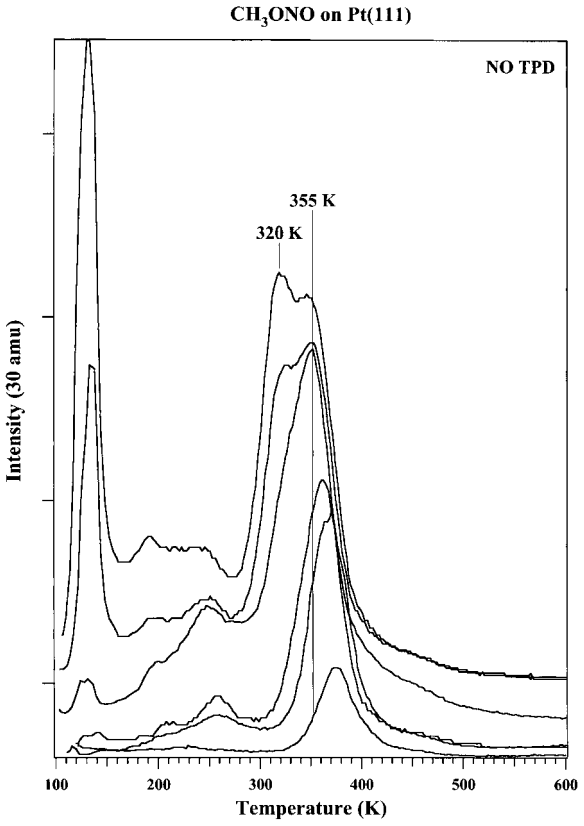

Fig. 4. NO TPD spectra obtained at 30 AMU after CH_3ONO exposures on the Pt(111) surface at 95 K. Exposures used were: 0.005, 0.010, 0.10, 0.20, 0.21, and 0.30 L.

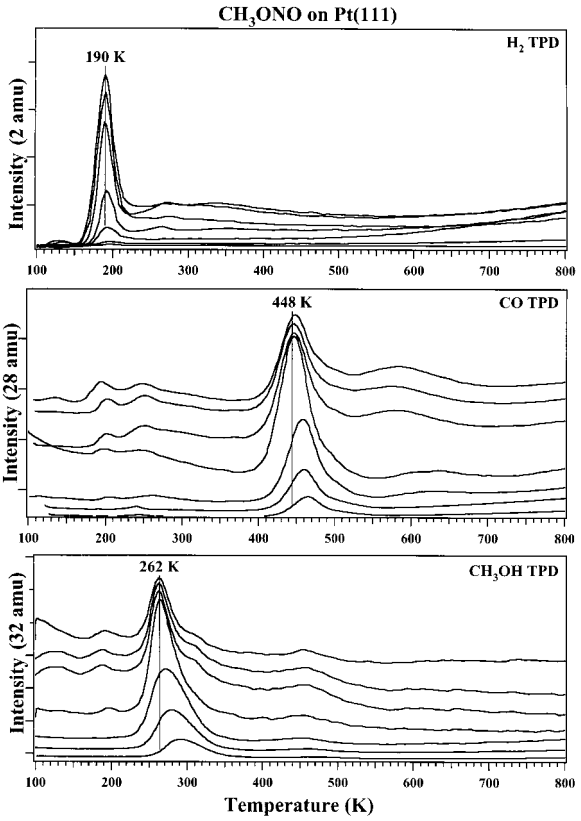

Fig. 5. TPD spectra obtained for 2, 28, and 32 AMU signals after CH_3ONO exposures on the Pt(111) surface. These spectra correspond primarily to desorption of H_2, CO, and CH_3OH products, respectively. Exposures used were: 0.005, 0.010, 0.10, 0.20, 0.21, 0.30, 0.35 L.

at the top of Fig. 5. H_2 TPD shows a single intense desorption feature at the lowest exposures at 290 K, which shifts to lower temperature with increasing coverage (the small features in the H_2 TPD spectra below 250 K and above 400 K are assigned to cracking fractions of higher mass species). Comparison of these spectra with the H_2 TPD spectra after H_2 exposure on Pt(111) [19] indicates that H_2 desorption from the decomposition of CH_3ONO is desorption rate-limited. The middle panel of Fig. 5 gives related TPD spectra monitored at 28 AMU showing primarily CO desorption. A decrease in CO desorption temperature from 460 K at the lowest exposures of CH_3ONO to 448 K at high coverages is observed (the low temperature features from 190 to 300 K

are assigned to contributions from CH_3OH and CH_2O cracking fractions, vide infra). Considering CO TPD spectra after CO exposures on Pt(111) [19] leads to the conclusion that CO desorption from the decomposition of CH_3ONO is also desorption rate-limited. A broad feature near 575 K in the CO TPD spectra for large CH_3ONO coverages is assigned to a reaction rate-limited process in the decomposition of hydrocarbon residues. The bottom panel of Fig. 5 shows TPD spectra obtained from the 32 AMU signal to monitor CH_3OH desorption after adsorption of CH_3ONO. At the lowest CH_3ONO coverages, no CH_3OH desorption is observed, but at higher coverages a single peak was seen at 190 K. This CH_3OH desorption temperature is very similar to that in CH_3OH TPD spectra after CH_3OH adsorption on Pt(111) [20,21], indicating that the primary CH_3OH desorption peak from decomposition of CH_3ONO is most likely desorption rate-limited.

In these TPD spectra, CO and H_2 evolution occurs at the lowest initial coverages, while CH_3OH only grows in at higher coverages, after the largest yield of CO and H_2 are observed. A competitive process between the production of CO and H_2 and methanol may be responsible. At low coverages, when the reactivity of the surface is highest, decomposition forms exclusively CO and H_2, while at higher coverages, coadsorbates inhibit complete decomposition of intermediates. The low temperature desorption of methanol strongly suggests that an important intermediate is methoxy, and that hydrogenation of methoxy to form methanol is a facile process.

AES spectra taken following each TPD run show significant carbon build up on the Pt(111) surface indicating that complete dissociation to carbon occurs for at least some of the methyl nitrite. No nitrogen or oxygen was detected by AES after TPD. We also used LEED in these investigations. Exposing the surface at 105 K to monolayer coverages of methyl nitrite, 0.18 L, only caused an increase in the diffuse background intensity for the (1×1) LEED pattern associated with the substrate, indicating that chemisorption of methyl nitrite occurs into a disordered adlayer phase.

3.2. HREELS of CD_3ONO

The top HREELS curve in Fig. 6 was obtained after an exposure of CD_3ONO that forms a monolayer coverage on the Pt(111) surface at 110 K. The HREELS spectrum of a monolayer of physisorbed methyl nitrite on Au(111) at 115 K [8] is shown for comparison in the bottom curve. In order to help assign the spectra on Pt(111), the vibrational assignments for CD_3ONO on Au(111) and in the gas phase are shown in Table 1 [17,22,23]. The Au(111) surface adsorbs methyl nitrite weakly (8 kcal/mol) and reversibly [8]. Based on this comparison we find that the HREELS spectra on Pt(111) at 110 K are not consistent with solely molecular CD_3ONO adsorption. The principle differences in the two spectra in Fig. 6 are the new peaks on Pt(111) at 1390 and 1595 cm^{-1}, along with an apparent shift of

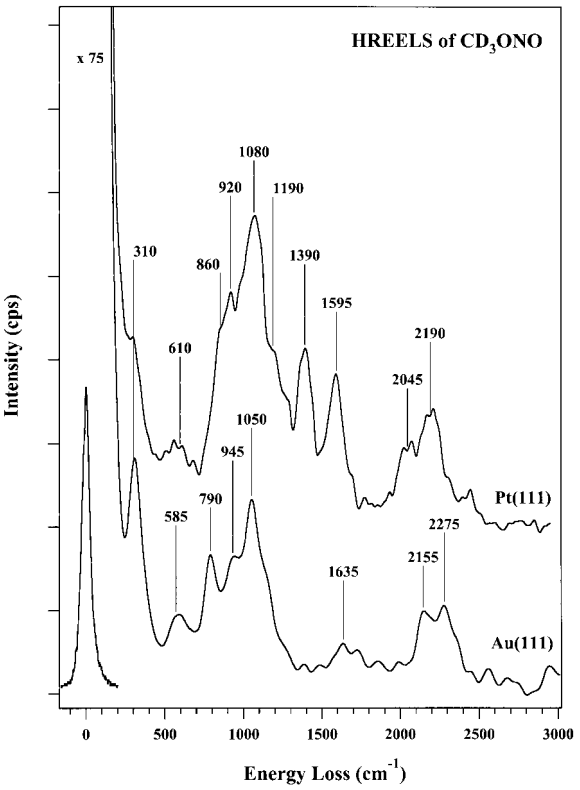

Fig. 6. HREELS spectra for near monolayer coverages of CH_3ONO adsorbed on Pt(111) and Au(111) [8] surfaces at 110 K.

Table 1
Assignment of the HREELS spectra for adsorbed methyl nitrite[a]

Assignment	CD_3ONO IR (solid) [17,22]				CD_3ONO on Pt(111) monolayer	CD_3ONO on Au(111) monolayer [8]
	cis		trans			
$\nu_{as}(C–D)$	2275	(3031)	2180[b]	(2913)	2190	2275
$\nu_{s}(C–D)$	2119[b]	(2952)	2038[b]	(2823)	2045	2155
$\nu(N=O)$	1610	(1613)	1664	(1665)		1635
$d_{as}(CD_3)$	1091[b]	(1452)	1055[b]	(1444)	1080	1050
$d_{s}(CD_3)$	1045	(1406)	1039[b]	(1422)		
$\nu(C–O)$	897[b]	(985)	950[b]	(1043)	920	945
$\nu(N–O)$	798	(838)	775	(806)		790
d(ONO)	595	(625)	551	(565)		585

[a] Values for CH_3ONO are shown in parentheses.
[b] Values from calculation.

the 2155 cm^{-1} peak to 2045 cm^{-1}, and the missing peaks at 310 and 790 cm^{-1}. The peaks at 1390 and 1595 cm^{-1} are considerably lower than the $\nu(N=O)$ modes previously observed for either gas phase or adsorbed methyl nitrite [8,9,17,22,23], and so we assign these peaks to $\nu(N=O)$ stretching vibrations of coadsorbed NO molecules [formed from the decomposition of CD_3ONO on Pt(111)]. These energy losses are 40–65 cm^{-1} lower than the $\nu(N=O)$ loss peaks for adsorbed molecular NO obtained by dosing NO on Pt(111) [18], but we attribute this to coadsorption effects. The other peaks for Pt(111) arise from molecular CD_3ONO on the surface. Several key features in this spectrum are also consistent with an assignment of methoxy (CD_3O) as a hydrocarbon fragment that accompanies NO formation from CD_3ONO decomposition.

HREELS spectra for several coverages of CD_3ONO on Pt(111) at 110 K are shown in Fig. 7. The bottom curve is from a dose giving a submonolayer coverage (≈0.25 ML) of CD_3ONO. This spectrum is difficult to assign using CD_3ONO modes. We can make an assignment based on the formation of a coadsorbed layer containing NO, methoxy (CD_3O), and CD_3ONO. Adsorbed NO gives losses at 1390 and 1595 cm^{-1} from the $\nu(N=O)$ stretching mode in two states of NO. As shown in Table 2 [24–29], d_3-methoxy on Ni(100) [27] is characterized by $\nu_s(CD_3)$ at 2059 cm^{-1}, $d_s(CD_3)$ at 1096 cm^{-1}, and $\nu(CO)$ at 986 cm^{-1}. We can attribute five loss peaks to methoxy

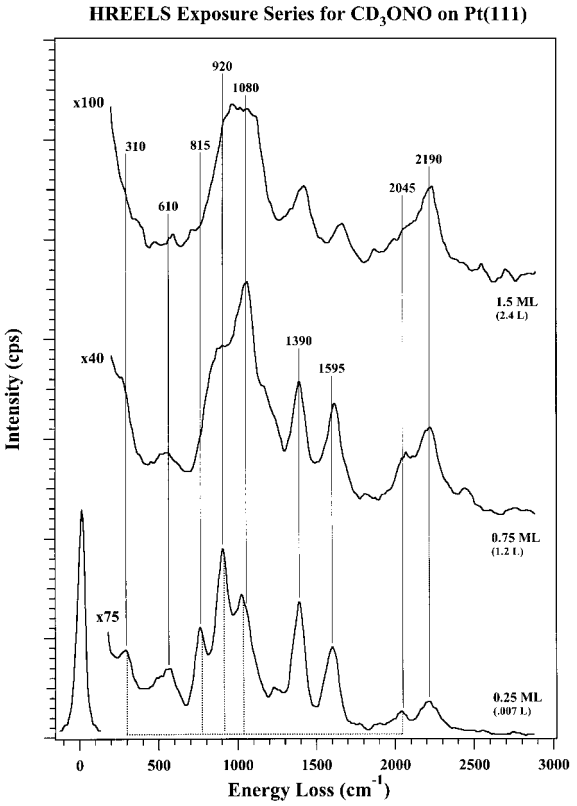

Fig. 7. HREELS spectra following exposures of CD_3ONO that form 0.25, 0.75, and 1.5 monolayers on the Pt(111) surface at 110 K.

in Fig. 7: $\nu(CD_3)$ at 2045 cm^{-1}, $d(CD_3)$ at 1080 cm^{-1}, $\nu(CO)$ at 920 cm^{-1}, $c(OCD_3)$ at 815 cm^{-1}, and $\nu(PtO)$ at 310 cm^{-1}. Methyl nitrite contributes intensity between 700 and 1200 cm^{-1},

Table 2
Vibrational bands (cm^{-1}) of CDO, CD_2O, CD_3O and CD_3OD

Species	Signal	Reference
CDO/Ru(001)-g2	550, 825, 980, 1160	[24,25]
CD_2O(g)	986, 1096, 2059	[26]
CD_2O/Ru(001)-g1	1025, 1190, 1640–1660, 2200–2250	[24,25]
CD_2O/Ru(001)-g2	620, 865, 1020, 1190, 2225	[24,25]
CD_3O/Ni(100)	986, 1096, 2059	[27]
CD_3O/Cu(110)	300, 990, 1100, 1950, 2060, 2190	[28]
CD_3OD/Ni(100)	834, 983, 1125, 2073, 2218, 2446	[27]
CD_3OD/(2×1)Pt(110)	560, 780, 990, 1100, 2070, 2235, 2410	[29]

and is solely responsible for the small peaks at 610 and 2190 cm^{-1}. Table 2 also shows that other possible surface species, such as CD_3OD, CD_2O, and CDO, have overlapping vibrational modes, and we cannot make a definitive assignment of the composition of the adlayer given the complications of such mixtures of species on the surface.

The spectra obtained at larger coverages are consistent with adding more molecular methyl nitrite on the surface. The n(CD_3) peak at 2190 cm^{-1} becomes much stronger than the peak at 2045 cm^{-1}, the relative intensity of the n(N=O) peaks decrease, and changes in the 700–1200 cm^{-1} loss region can be related to increases in peaks that resemble the spectrum of methyl nitrite on Au(111). Difference spectra reveal these changes more clearly, but these are not reproduced here. The partial decomposition of methyl nitrite under our conditions and the rather complex coadsorbed layer thus formed make it impossible for us to conclude anything about the adsorption geometry of molecularly adsorbed methyl nitrite on Pt(111). It has been proposed that methyl nitrite adsorbs on Au(111) [8] and Ag(111) [9] in a geometry in which the O–N=O plane is parallel with the surface.

The warm-up series of HREELS spectra shown in Fig. 8 begins with a dose of methyl nitrite corresponding to nearly monolayer coverage on Pt(111) at 110 K. This curve is the same as that shown in Fig. 6 and discussed above. Heating to 130 K causes desorption of any physisorbed methyl nitrite, and the HREELS spectra show an overall decrease in loss peak intensities other than those for NO that is consistent with some methyl nitrite

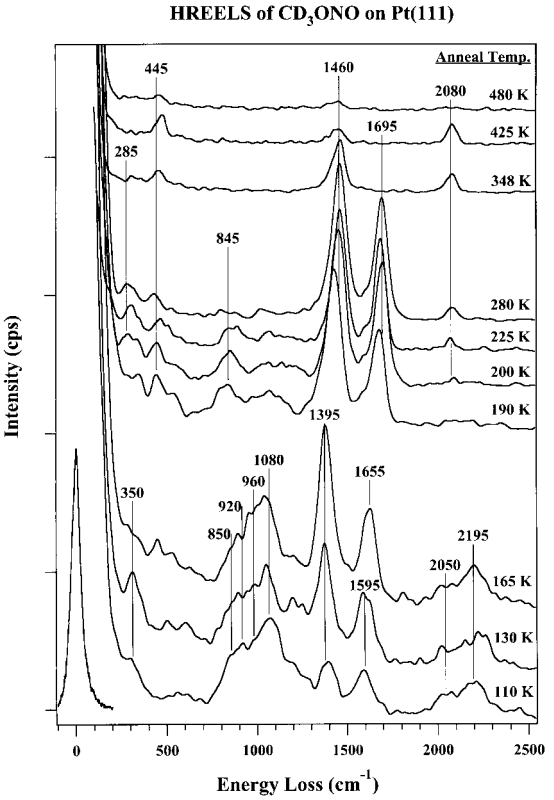

Fig. 8. HREELS warm-up series after a dose of CD_3ONO which forms 1.2 monolayers on the Pt(111) surface at 110 K.

desorption. The n(C–D) peak that we have assigned to methoxy also decreases in relative intensity and the higher energy loss peak shifts to about 2250 cm^{-1}. Warming the surface to 165 K has very little effect on the spectrum except that the high energy n(N=O) peak at 1595 cm^{-1} shifts

to 1655 cm^{-1}. We interpret this shift to indicate that there is no longer any adsorbed methyl nitrite on the surface. Methanol evolution occurs in TPD at 190 K, and heating to 190 K causes large changes in HREELS. The intensity in the 700–1200 cm^{-1} loss region is strongly reduced, the NO loss peaks shift to 1460 and 1695 cm^{-1}, and the n(C–D) peaks disappear. In Fig. 8, we never observe vibrational peaks that cleanly identify adsorbed methoxy, and we conclude that methoxy intermediates must be relatively unstable (reactive) on the surface. The adsorbed layer at 190 K consists of coadsorbed NO, H, and some hydrocarbon, either formaldehyde (H_2CO) or formyl (HCO). No CO has yet been formed. Above 200 K a CO peak grows in until 280 K concurrently with desorption of H_2 and a small amount of formaldehyde. The two small peaks at 285 and 445 cm^{-1} can be associated with low frequency modes of bent NO on the Pt(111) surface [18]. At 280 K, only CO and NO remain on the surface. The adsorbed CO has a loss peak at 2080 cm^{-1}. Heating to 348 K desorbs most of the NO, leaving only the most strongly bound NO that has n(N=O) at 1460 cm^{-1}, and heating to 425 K effectively removes all of the NO. The CO product is finally removed after heating to 480 K, leaving a relatively clean surface (we did see a small amount of surface carbon in AES, however).

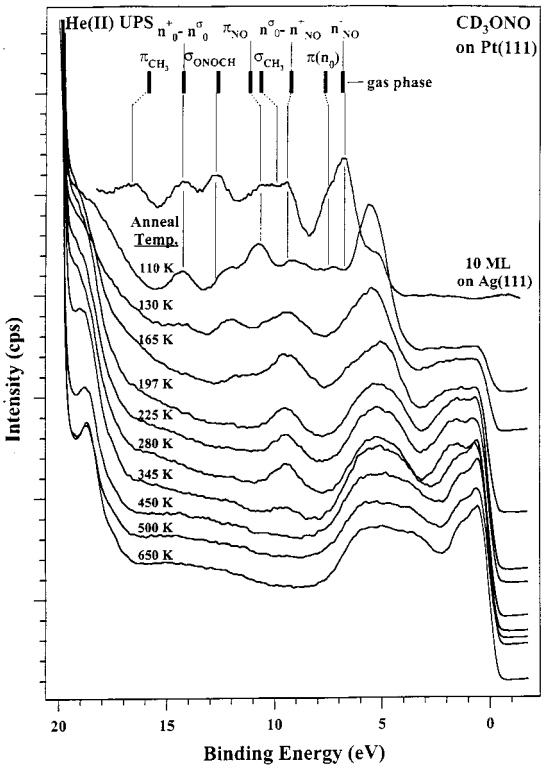

Fig. 9. Warm-up series using He(II) UPS after exposure of CD_3ONO to form 1.2 monolayers on Pt(111) at 110 K. The top spectra was obtained after dosing, without warming. The dark bars at the top of the figure correspond to peaks obtained from UPS spectra of gas phase CH_3ONO [24] uniformly shifted down in energy by 4.2 eV to account for final state screening effects.

3.3. UPS of CD_3ONO

He(II) ultraviolet photoelectron (UPS) spectra for a coverage of CD_3ONO near one monolayer on Pt(111) after various warm-up temperatures are shown in Fig. 9. The vertical bars at the top of Fig. 9 are the peak positions of gas phase CH_3ONO [30] that have been uniformly shifted by 4.2 eV to lower binding energy to account for relaxation effects and to give the best alignment with the condensed phase spectrum of CD_3ONO on Ag(111) (top curve) [9]. The peak positions and orbital assignments are listed in Table 3. Oddly, the p_{CH_3} orbital apparently undergoes an additional differential shift of 0.3 eV between the gas and condensed phase. The top curve in our new data was obtained after dosing CD_3ONO on Pt(111) at 110 K. In addition to the Pt d-band intensity between 0 and 7 eV, this spectrum shows evidence for the presence of molecularly adsorbed methyl nitrite under these conditions, but we were unable to give a good account of all of the positions and intensities of the observed photoemission peaks by utilizing small shifts of the molecular CH_3ONO peaks. Primarily, we have additional intensity at 5.7, 8.0, and 10.8 eV that is unaccounted for by CH_3ONO. This UPS spectrum provides key supporting information to our assignment using HREELS that decomposition of CD_3ONO occurs upon adsorption on Pt(111) at 110 K (because of large changes that can occur in mode intensities and frequencies in HREELS due to strong chemisorption and the dipole selection rule). The formation of methoxy, and possibly

Table 3
Orbital binding energies from UPS for CD_3ONO[a]

Orbital	BE (eV)		
	Gas phase [31]	10 ML on Ag(111)	1 ML on Pt(111)
n^-_{NO}	11.0	6.8	5.5
$p(n_0)$	11.8	7.5	6.1
$ns_0 - n^+_{NO}$	13.4	9.5	7.3
s_{CD_3}	14.8	10.5	8.6
p_{NO}	15.3	11.4	9.3
s_{ONOCH}	16.8	12.9	10.8
$n^+_{NO} + ns_0$	18.4	14.1	12.1
p_{CH_3}	20.0	16.8	14.3

[a] Binding energies for the gas phase are referenced to $E_{vac}=0$ and those for the adsorbed phase are referenced to $E_F=0$.

methanol, would be consistent with this UPS spectrum, as shown in Table 4 [31–39].

The UPS warm-up series also helps to define the temperatures at which reactions occur. Heating to 130 K causes a reduction in the coverage of methyl nitrite as shown by the increase in the Pt d-band intensity at the Fermi level (E_F) and a large reduction in the intensity of all peaks associated with CD_3ONO. By 165 K, there are no features attributable to CD_3ONO remaining, which agrees well with the HREELS results. Adsorbed NO causes a peak at 9.3 eV that arises from the NO (1p) level [40], and some hydrocarbon intermediate must be responsible for additional intensity including peaks at 11.7 and 5.0 eV. Annealing to 197 K sharpens the peak associated with the NO (1p) level at 9.3 eV, and any other adsorbed intermediates have only weak intensity in the Pt d-band region. Heating to 345 K desorbs most of the NO, and the broad feature at about 9 eV has some contribution from the 1p and 5s states of CO [41]. Heating to 450 K forms a relatively clean Pt(111) surface.

Table 4
Orbital binding energies (eV) from UPS

Species	Signal	Reference
para-CH_2O/Cu(110)	6.2, 9.3, 12.1, 15.4	[31]
CH_2O/Cu(110)	5.7, 9.3, 11.2, 16.0	[31]
CH_2O/Pd(100)	5.2, 9.1, —	[32]
CH_3O/Cu(110)	5.5, 8.5, 15.5	[33]
	5.5, 9.5, 15.5	[34]
CH_3O/Ni(111)	5.3, 9.5, —	[35]
CH_3O/Cr(110)	6.6, 10.7, 17.3	[36]
CH_3OH/Pt(111)	5.9, 7.7, 10.3, 12.7, —	[37]
CH_3OH/Ni(111)	5.2, 7.0, 9.5, 12.0, —	[35]
CH_3OH(ads)/Cu(100)	5.8, 7.6, 10.1, 12.3, —	[38]
CH_3OH(ads)/Pd(100)	4.9, 6.7, 9.2, 11.4, —	[39]
CH_3OH(ads)/Cr(110)	—, 6.6, 10.7, 17.3, —	[36]

From the onset of secondary electrons in the He(I) data, we determined that the work function of clean Pt(111) was 5.57 eV. Adsorbing a coverage of CD_3ONO near one monolayer on Pt(111) at 110 K, corresponding to the top curve in Fig. 9, reduces the work function by 1.65 eV.

4. Discussion

Methyl nitrite (CH_3ONO) is a very reactive molecule on the Pt(111) surface. Some dissociation occurs even at 110 K. The chemisorbed monolayer undergoes complete dissociation at very low temperatures (below 165 K); no molecular desorption is observed from the chemisorbed state. Thus, methyl nitrite is more reactive on Pt(111) than NO_2 [42] or CH_3NO_2 [12]. This is due to the weak CH_3O–NO bond in methyl nitrite, where D(O–NO)=42 kcal/mol in the gas phase [7]. The bond dissociation energy is greatly reduced in the chemisorbed layer since the dissociation products CH_3O and NO are both strongly chemisorbed, and only small (perhaps intrinsic) barriers to reaction inhibit cleavage of the O–NO bond. Reaction of adsorbed methyl nitrite on Pt(111) leads pri-

marily to production of NO, CO, and H_2 in TPD. Some methanol desorption is also seen, and it is likely that this product arises from the hydrogenation of a methoxy (CH_3O) intermediate. The dependence of the amounts of CO, NO, and CH_3OH evolved as a function of CH_3ONO initial coverage indicates that competitive processes are at work at all but the lowest coverages. In the uptake plot shown in Fig. 3, NO production steadily increases with increasing exposures of methyl nitrite, but CO and H_2 production peak at low CH_3ONO coverage ($\theta_{CH_3ONO} \sim 0.15$ ML). This maximum in the CO and H_2 yield is correlated to methanol desorption. In the absence of a sufficiently large concentration of coadsorbates when $\theta_{CH_3ONO} < 0.15$ ML, methoxy and any subsequent intermediates present after O–NO bond cleavage completely dissociate on Pt(111) to yield CO and H_2. As the initial CH_3ONO coverage increases and coadsorbed CO, H, and unreacted CH_3ONO inhibit reactions on the surface, the barrier to decomposition of methoxy increases and hydrogenation to form methanol becomes a competitive reaction channel. Methanol produced in this manner desorbs in a desorption rate-limited peak at low temperatures (190 K) [20]. The H_2 and CO products desorb at 300 and 400 K, respectively, in desorption rate-limited peaks [19].

Both HREELS and UPS confirm a high reactivity of methyl nitrite and methoxy species. HREELS and UPS show that by 165 K there is no longer any CD_3ONO on the surface. The NO loss intensity in HREELS increases by 80% at 130 K and reaches its maximum value by 165 K. This loss intensity indicates that $\approx$25% of the CD_3ONO initially decomposed upon adsorption at 110 K and that decomposition of CD_3ONO is complete at 165 K. Methyl nitrite dissociates to form chemisorbed NO on the surface and cleavage of the O–NO bond forms at least a transient methoxy intermediate, and probably a stable adsorbed methoxy species. This would be consistent with the HREELS spectra at low coverage. In UPS, the 12.2 eV peak that arises after heating to 130 K is consistent with a methoxy intermediate or chemisorbed methanol [36], and the weak feature at 11.4 eV BE after heating to 160 K can be assigned to a small concentration of some other hydrocarbon intermediate (H_2CO or HCO) [31] that is fairly cleanly converted to CO and H_2 at higher temperatures. No features in either HREELS or UPS can be assigned to methoxy species at 190 K, and so any surface bound methoxy has decomposed by this temperature.

A few other details of the decomposition mechanism emerge from further consideration of the HREELS warm-up spectra. Desorption of methanol at 190 K is probably responsible for the shift of the ν(N=O) peaks to 1460 and 1695 cm^{-1}, which are the same values obtained for NO adsorbed on the Pt(111) surface after NO exposure [18]. Our picture is that dissociation of methyl nitrite yields chemisorbed NO in two sites and by 200 K methoxy has either decomposed to form H_2CO and/or HCO or has hydrogenated and desorbed as methanol. At this temperature, some of the hydrocarbon fragments have been removed from the surface as methanol, but what remains decomposes to form CO on the surface. HREELS shows that some hydrocarbon intermediate (that is not methoxy) exists on the surface up to at least 280 K. By 280 K, the loss peaks between 800 and 1200 cm^{-1} disappeared and a small loss peak at 2080 cm^{-1} appeared that is a signature for adsorbed CO [43]. It would be helpful to assign the surface species formed from methoxy decomposition, but this is complicated by the low coverage, the presence of potentially overlapping ν(N=O) peaks, and the possibility for rehybridization of the carbonyl group. Previous HREELS experiments involving formaldehyde (H_2CO) on Ag(111) [29] assigned a ν_s(OCO) stretch at 965 cm^{-1} and a ν_{as}(OCO) stretch at 1120 cm^{-1} for formaldehyde polymerized (paraformaldehyde) on the surface, and this is inconsistent with our spectra. Even though only a small formaldehyde product was observed in TPD at $\sim$250 K, we would expect formaldehyde to decompose to CO and H_2 on Pt(111) [44,45] rather than desorb if it were a product of the reaction. In any event, the loss peaks between 800 and 1200 cm^{-1} in HREELS disappear at approximately the same temperature that desorption of formaldehyde occurs. As the temperature increases further, NO desorbs from the surface, first from the more weakly bound atop sites [18] by 350 K, and then from the more

strongly bound three-fold hollow sites at 425 K. Essentially only CO remains on the surface at 425 K, and then CO desorbs by 480 K which is consistent with the TPD results.

We can utilize the desorption energies and reaction activation energies from TPD and our understanding of the reaction mechanism to develop some insight into the thermochemistry of the reactions of methyl nitrite adsorbed on Pt(111). Fig. 10 shows a schematic diagram of our proposed energetics. The energy zero is the heat of formation of the elements in their standard states, i.e. $D\!H^{\circ}_{f,300}(H_{2(g)}) = D\!H^{\circ}_{f,300}(Pt_{(s)}) = 0$. Mass balance requires that we consider the heats of formation of the coadsorbed products required by stoichiometry. For the stable gas phase molecules, $D\!H^{\circ}_{f,300}(CH_3ONO_{(g)}) = -16.9$ kcal/mol, $D\!H^{\circ}_{f,300}(CO_{(g)}) = -26.4$ kcal/mol, and $D\!H^{\circ}_{f,300}(NO_{(g)}) = 21.6$ kcal/mol [46]. Known heats of adsorption for CO (32 kcal/mol [47]), NO (19 kcal/mol [48]), and H_2 (19 kcal/mol [49]) allow us to calculate for the adsorbed species $D\!H^{\circ}_{f,300}(CO_{(a)}) = -58.4$ kcal/mol, $D\!H^{\circ}_{f,300}(NO_{(a)}) = 2.6$ kcal/mol, and $D\!H^{\circ}_{f,300}(H_{(a)}) = -10$ kcal/mol [50]. To finish constructing the diagram, we need to know heats of formation for adsorbed CH_3ONO and any hydrocarbon intermediates formed. We can place an upper limit of $D\!H^{\circ}_{f,300}(CH_3ONO_{(a)}) = -33.2$ kcal/mol because we know that molecular desorption occurs at 267 K with a desorption activation energy of 16.3 kcal/mol on a Pt–Sn alloy which is less reactive than Pt(111) [10,11]. We estimate the value of $D\!H^{\circ}_{f,300}(CH_3O_{(a)}) = -39.0$ kcal/mol by subtracting the methoxy adsorption energy, taken as 42.5 kcal/mol by using one-half the bond energy of adsorbed oxygen atoms on Pt(111) where $D(Pt–O) = 85$ kcal/mol [51], from $D\!H^{\circ}_{f,300}(CH_3O_{(g)}) = 3.5$ kcal/mol [50]. We also concluded that some other hydrocarbon intermediate was formed on the surface prior to the formation of CO, but we are unable to reliably estimate the formation energy of this species at this time (primarily due to a lack of information on the energetics of free radical excited states [50]). The overall reaction that yields the major gas phase products depicted here is endothermic by 12.1 kcal/mol. The barrier to decompose adsorbed CH_3ONO is about 7 kcal/mol because some decomposition occurs upon adsorption at 110 K. An upper limit for the barrier to decompose methoxy is 11 kcal/mol because of the desorption rate-limited appearance of methanol in TPD, which can only be formed if dehydrogenation of methoxy occurs. The other hydrocarbon intermediate is more stable than methoxy because CO is not observed in HREELS annealing studies until about 225 K. We estimate a barrier of about 17 kcal/mol for this process. Obviously the reaction is most exothermic to form the adsorbed products, and this indeed is the driving force for

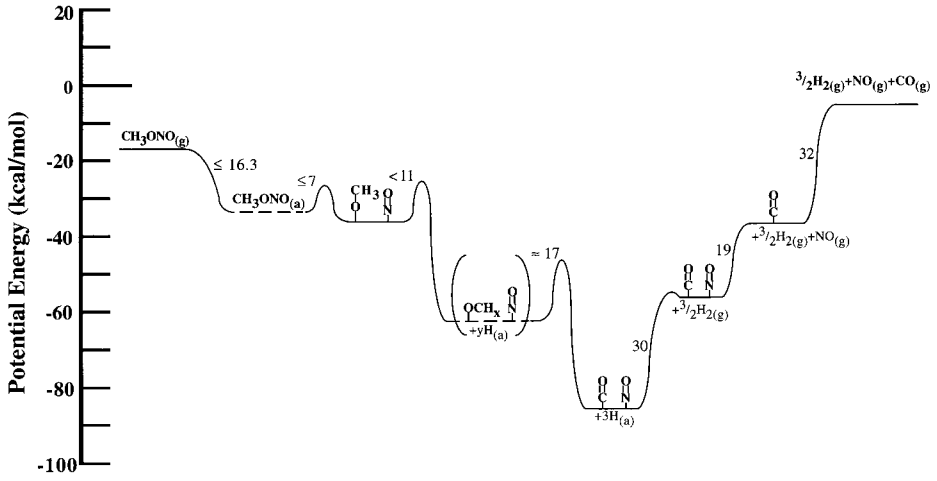

Fig. 10. Energetics for the reaction of methyl nitrite on Pt(111).

the high reactivity of CH_3ONO on Pt(111) that we observe. The endothermic processes that lead to desorption of the small molecule products in TPD are driven by entropic effects.

Our results lead naturally to some conclusions about the reactivity of methoxy species on Pt(111), which in the past have been impossible to obtain without surface defects or coadsorbed O adatoms because CH_3OH does not dissociatively chemisorb on Pt(111) [20,52]. We conclude that methoxy is quite reactive, with a barrier to decomposition below 11 kcal/mol, and decomposition leads almost exclusively to CO and H_2. This chemistry is similar to that in previous studies of methanol on defective Pt(111) substrates [21,53–56], where TPD of submonolayer coverages of methanol desorbed only CO and H_2. We also conclude that hydrogenation of methoxy is a facile process, with a barrier less than 11 kcal/mol, since CH_3OH is produced below 190 K.

Finally, we mention that we have proposed using methyl nitrite as an adsorbed precursor to cleanly form methoxy at relatively low temperature on reactive metal surfaces [10]. Studies of the chemistry of CH_3ONO on the two Sn/Pt(111) surface alloys have been carried out [11]. About 60–70% of the chemisorbed monolayer of methyl nitrite undergoes decomposition depending on which surface alloy is used, but CO and H_2 do not appear as gas phase products from methyl nitrite reaction. Instead, these alloys have a high selectivity for desorbing methanol and formaldehyde. We observe that the stability of surface methoxy is enhanced on the Sn/Pt(111) surface alloys compared to that on Pt(111).

5. Conclusion

Methyl nitrite undergoes facile dissociation on Pt(111). The chemisorbed monolayer completely decomposes during TPD, and HREELS and UPS show that some dissociation of methyl nitrite occurs upon adsorption on Pt(111) at 110 K. At low CD_3ONO coverages, when the surface reactivity is highest, reactions during TPD only produce gas phase NO, CO and H_2, while at higher coverages, as the concentrations of coadsorbates increase and deactivate the surface, gas phase methanol is an important product. Adsorbed NO is formed from nascent CD_3ONO dissociation, and we propose that an adsorbed methoxy intermediate is also formed. Dehydrogenation of methoxy forms a hydrocarbon species which ultimately produces CO and H_2 desorption and hydrogenation forms methanol which desorbs. Methyl nitrite adsorption allows us to make several new observations about the reactivity of methoxy on defect-free Pt(111) surfaces. Dehydrogenation and hydrogenation to form methanol are both relatively facile processes with barriers below 11 kcal/mol.

Acknowledgements

This work was partially supported by the Army Research Office. The authors would like to thank J. Wang for synthesizing the methyl nitrite sample and J.M. White for making his results available to us prior to their publication. J.W.P. gratefully thanks the Department of Education for a graduate research fellowship.

References

[1] A.M. Wodtke, E.J. Hintsa, Y.T. Lee, J. Chem. Phys. 84 (1986) 1044.
[2] D. Dahlgren, J.C. Hemminger, Surf. Sci. 123 (1982) L739.
[3] J. Segner, W. Vielhaber, G. Ertl, Israel J. Chem. 22 (1982) 375.
[4] R. Engelke, W.L. Earl, C.M. Rohlfing, J. Chem. Phys. 84 (1986) 142.
[5] R. Engelke, W.L. Earl, C.M. Rohlfing, J. Chem. Phys. 90 (1986) 545.
[6] A. Perche, J.C. Tricot, M. Lucquin, J. Chem. Res. (1979) 1555.
[7] M.J.S. Dewar, J.R. Ritchie, J. Alster, J. Am. Chem. Soc. 50 (1985) 1031.
[8] J. Wang, N. Saliba, B. Bansenaur, B.E. Koel, J. Phys. Chem., in press.
[9] L.A. Pressley, E.D. Pylant, J.M. White, Surf. Sci. 367 (1996) 1.
[10] J.W. Peck, D. Mahon, D. Beck, B.E. Koel, J. Phys. Chem. B 102 (1998) 3321.
[11] J.W. Peck, D. Mahon, D. Beck, B.E. Koel, submitted to Surf. Sci. 410, this issue.

[12] N. Saliba, J. Wang, B. Bansenaur, B.E. Koel, Surf. Sci. 389 (1997) 147.
[13] J.E. Katz, P.W. Davies, J.E. Crowell, G.A. Somorjai, Rev. Sci. Instrum. 53 (1982) 785.
[14] C. Xu, Y.-L. Tsai, B.E. Koel, J. Phys. Chem. 98 (1994) 585.
[15] C. Xu, B.E. Koel, Surf. Sci. 292 (1993) L803.
[16] F.L. Rook, J. Chem. Eng. Data 27 (1982) 72.
[17] P.N. Ghosh, Hs.H. Gunthard, Spectrochim. Acta 37A (1981) 347.
[18] C. Xu, B.E. Koel, Surf. Sci. 310 (1994) 198.
[19] M.T. Paffett, S.C. Gebhard, R.G. Windham, B.E. Koel, J. Phys. Chem. 94 (1990) 6831.
[20] C. Panja, N. Saliba, B.E. Koel, Surf. Sci. 395 (1998) 248.
[21] B.A. Sexton, Surf. Sci. 102 (1981) 271.
[22] M. Bodenbinder, S.E. Ulic, H. Willner, J. Phys. Chem. 98 (1994) 6441.
[23] J.E. Fieberg, J.M. White, J. Vac. Sci. Technol., A (1997) May/June.
[24] A.B. Anton, J.E. Parmeter, W.H. Weinberg, J. Am. Chem. Soc. 107 (1985) 5558.
[25] A.B. Anton, J.E. Parmeter, W.H. Weinberg, J. Am. Chem. Soc. 108 (1986) 1827.
[26] T. Nakanaga, S. Kondo, S. Saëki, J. Chem. Phys. 76 (1982) 3860.
[27] J.S. Huberty, R.J. Madix, Surf. Sci. 360 (1996) 144.
[28] B.A. Sexton, Surf. Sci. 88 (1979) 299.
[29] K. Franaszczuk, E. Herrero, P. Zelenay, A. Wieckowski, J. Phys. Chem. 96 (1992) 8509.
[30] H. Bergmann, H. Bock, Z. Naturforsch. 30B (1975) 629.
[31] B.A. Sexton, A.E. Hughes, N.R. Avery, Surf. Sci. 155 (1985) 366.
[32] F. Solymosi, A. Berkó, Z. Tóth, Surf. Sci. 285 (1993) 197.
[33] M. Bowker, R.J. Madix, Surf. Sci. 95 (1980) 190.
[34] T.A. Carlson, P.A. Agron, T.M. Thomas, F.A. Grimm, J. Electron Spectrosc. Relat. Phenom. 23 (1981) 13.
[35] G.W. Rubloff, J.E. Demuth, J. Vac. Sci. Technol. 14 (1977) 419.
[36] N.D. Shinn, Surf. Sci. 278 (1992) 157.
[37] D.H. Ehlers, A. Spitzer, H. Lüth, Surf. Sci. 160 (1985) 57.
[38] B.A. Sexton, A.E. Hughes, Surf. Sci. 140 (1984) 227.
[39] K. Christmann, J.E. Demuth, J. Chem. Phys. 76 (1982) 6308.
[40] M.E. Bartram, B.E. Koel, Surf. Sci. 219 (1989) 467.
[41] B.E. Koel, D.E. Peebles, J.M. White, J. Vac. Sci. Technol. 20 (1982) 889.
[42] M.E. Bartram, R.G. Windham, B.E. Koel, Langmuir 4 (1988) 240.
[43] B.J. Bandy, M.A. Chesters, P. Hollins, J. Pritchard, N. Sheppard, J. Mol. Struct. 80 (1982) 203.
[44] M.A. Henderson, G.E. Mitchell, J.M. White, Surf. Sci. 188 (1987) 206.
[45] J.T. Yates, T.E. Madey, M.J. Dresser, J. Catal. 30 (1973) 260.
[46] S.W. Benson, Thermochemical Kinetics, Wiley, New York, 1976.
[47] G. Ertl, M. Neumann, K.M. Streit, Surf. Sci. 64 (1977) 393.
[48] M.E. Bartram, B.E. Koel, E.A. Carter, Surf. Sci. 219 (1989) 467.
[49] B. Poelsema, G. Mechtersheimer, G. Comsa, Surf. Sci. 111 (1981) 519.
[50] E.A. Carter, B.E. Koel, Surf. Sci. 226 (1990) 339.
[51] D.H. Parker, M.E. Bartram, B.E. Koel, Surf. Sci. 217 (1989) 489.
[52] K.D. Gibson, L.H. Dubois, Surf. Sci. 223 (1990) 59.
[53] I.E. Wachs, R.J. Madix, Surf. Sci. 76 (1978) 531.
[54] I.E. Wachs, R.J. Madix, J. Catal. 53 (1978) 208.
[55] B.A. Sexton, Surf. Sci. 102 (1981) 271.
[56] B.A. Sexton, K.D. Rendulic, A.E. Hughes, Surf. Sci. 121 (1982) 181.